Department of Geosciences and Geography
Series of publications A131
University of Helsinki

Multisource remote sensing framework for monitoring soil, crop and land-surface processes in smallholder farms

Ashfak Mahmud

ACADEMIC DISSERTATION
To be presented, with the permission of Faculty of Science of the University of Helsinki, for public examination in Karolina Eskelin Hall (U3032), University main building, on 2 October 2026, at 12 noon.

Helsinki 2026

Pre-examiners

Dr. Sirpa Thessler, Natural Resources Institute Finland (Luke)

Professor Tobias Benedikt Hank, Ludwig-Maximilians-Universität München

Custos

Professor Petri Pellikka, University of Helsinki

Supervisors

Docent Janne Heiskanen, University of Helsinki

Dr. Juuso Tuure, University of Helsinki

Professor Petri Pellikka, University of Helsinki

Opponent

Associate Professor Anton Vrieling, University of Twente

© Ashfak Mahmud (Synopsis)
© Elsevier (Article I)
© Elsevier (Article II)

Cover Image: Euliud Kinyanjui, Ramani Geosystems

ISBN 978-952-84-2604-2 (paperback)
ISBN 978-952-84-2605-9 (PDF)
ISSN 1798-7911 (print)
ISSN-L 1798-7911 (PDF)

Unigrafia / PunaMusta
Joensuu 2026

This thesis is dedicated to the memory of my uncle, Professor Muhammad Kamaluddin (1953–2005), whose life, values, and example remained a constant source of inspiration throughout this journey.

Abstract

Smallholder cropping systems in East Africa are highly heterogeneous, with strong variation in soils, crop development, vegetation cover, and thermal conditions across short distances and contrasting agroecological zones. This spatial and temporal complexity makes agricultural monitoring difficult using conventional field methods alone, especially where repeated and scalable assessment is needed.

The thesis brings together three articles that collectively examine the monitoring of soil, crop, and land-surface dynamics in smallholder cropping systems. Article **I** examined the potential of proximal hyperspectral sensing for rapid estimation of soil organic carbon and soil nitrogen under field-laboratory conditions. Article **II** investigated the use of field camera imagery for monitoring maize phenology, crop biophysical traits, and agroclimatic responses across agroecological zones. Article **III** developed a multiscale approach for analysing fractional vegetation cover and its relationship with land surface temperature using field, UAV, and satellite imagery.

The results showed that soil organic carbon was estimated more accurately than soil nitrogen, and that broad spectral coverage, especially the shortwave infrared region, improved model performance. Field camera-derived greenness time series reflected maize biophysical traits and agroclimatic fluctuations and enabled accurate detection of key maize phenological stages. The multiscale analysis showed that UAV-derived vegetation cover can be transferred successfully to satellite scale, and that vegetation cover was consistently negatively related to land surface temperature, with stronger cooling effects under warmer and drier conditions. Across agroecological zones, a 10-percentage-point increase in vegetation cover was associated with roughly 0.7–3.1 °C lower land surface temperature.

Taken together, the findings showed that effective monitoring of heterogeneous smallholder systems requires combining methods that differ in scale and purpose: spectroscopy for soil assessment, field cameras for continuous crop monitoring, and UAV–satellite integration for landscape-scale vegetation and thermal analysis. The thesis contributes to remote sensing of smallholder agriculture by advancing a more integrated and scalable monitoring framework for fragmented agricultural landscapes.

Acknowledgements

When I moved to Finland, I did not know a single person here. Looking back now, I feel deeply grateful that this journey has become easier by the support, kindness, and encouragement of so many people. This doctoral journey would not have been possible without them.

First and foremost, I would like to express my sincere gratitude to my supervisors, Dr. Janne Heiskanen, Dr. Juuso Tuure, and Professor Petri Pellikka. Dr. Janne, I consider myself truly fortunate to have a kind, encouraging, and supportive supervisor like you. Thank you for always welcoming me with a warm smile and having my back during difficult times. Dr. Juuso, you have been an important part of this PhD journey. Your constant support, especially your agricultural expertise and help with data-related matters, has been invaluable. I deeply appreciated how you were always just one email away whenever I needed guidance. Professor Petri, thank you for your continuous support during my PhD. Your advice and help with practical matters were crucial for bringing this PhD to completion. My sincere thanks go to my thesis committee members, Professor Janne Soininen and Associate Professor Antti Lajunen. Thank you for your valuable guidance and constructive comments during my doctoral studies.

My sincere thanks go to my colleagues at the department specially in ECHOLAB and the Tree-D research group for your support, encouragement, and the many valuable interactions along the way. Ian, you were incredibly helpful when I first moved here. Sharing an office with you in the beginning made my transition so much easier, and I truly appreciated how patiently and dedicatedly you helped me with all the practicalities of getting started. Ilja, you have been always ready to extend a helping hand whenever it was needed. I also greatly appreciated the time we spent at AGU in New Orleans. Pauline, thank you for always being so kind, and ready to help whenever I needed, sometimes even without asking. Zhaozhi, thank you for the friendship and laughter that started at Hyytiälä Station and made this journey lighter and more memorable. I would like to warmly thank Sumaiya and Dibash for the good memories, shared experiences, and the opportunity to work together. I would also like to sincerely thank the following people for their support, kindness, and the many memorable moments shared along the way: Eduardo, Iris,

Morice, Antti, Veronica, Jonathan, Zhimin, Elisa, Amanda, Hari, Erone, Sara, Kifle, Ying, Juzheng, Matti, Filagot, Saana, and Tom. I would also like to sincerely thank Nadja Den Besten for being such an important part of my academic journey. Since my MSc internship at Planet Labs, I have learned so much from you, and you have always made the effort to check in on me which made this PhD journey a little easier.

I would also like to express my sincere gratitude to the members of Ekenäs Cricket Club. Cricket was a constant source of strength, balance, and belonging during my years in Finland. My sincere gratitude goes to the Chittagong University Scientific Society and CUSS YouthMappers, organizations that have long remained close to my heart. I would like to express my heartfelt gratitude to my dear friends beyond academia. In Finland, I am especially grateful to Pritom, Punom, Monti, Adrita, Mohima, Sajjad bhai and Rafeul for their friendship and weekend adda. I also deeply value my friendship with Khadiza, Esha, Adil, Sraboni, Sharmin, Moon, Salar, Abdullah, Muhammad, Rhydwan, Robin, Mojammel, whose friendship carried me through this PhD journey. Khadiza, thank you for being a shadow through my ups and downs and a true source of energy during the most difficult days. My deepest thanks go to my family, whose endless understanding, love, and support carried me through my doctoral studies and continue to give me strength for the future. A heartfelt thank you to my cousin Belal bhaiya and Nasrin bhabi for your constant support and for always checking in to make sure I am doing okay. Your care and kindness mean so much to me.

Index

Abstract iv

Acknowledgements v

List of original publications ix

Author contribution x

List of figures xi

List of tables xii

List of abbreviations xiii

1 Introduction 1

1.1 Smallholder cropping systems and regenerative agriculture 1

1.2 The need for scalable monitoring of soil, crop, and land-surface processes. 2

1.3 Remote sensing as a tool for agricultural monitoring 3

1.4 Research gaps and objectives 4

2 Materials and methods 6

2.1 Study area and agroecological setting 6

2.2 Overview of datasets and sensing platforms 8

2.2.1 Agroclimatic datasets 8

2.2.2 Biophysical datasets 8

2.2.3 Proximal hyperspectral datasets 8

2.2.4 Field camera images 9

2.2.5 UAV images 9

2.2.6 Satellite images 10

2.3 Soil spectroscopy for organic carbon and nitrogen determination 10

2.4 Monitoring crop phenology, biophysical traits, and agroclimatic variability using field cameras 12

2.5 Multiscale analysis of fractional vegetation cover and land surface temperature 13

3 Results and discussion 14

3.1 Estimation of soil organic carbon and nitrogen 14

3.2 Monitoring of crop phenology, biophysical and agroclimatic variables 15
3.3 Multiscale analysis of fractional vegetation cover and land surface temperature 16
4 Synthesis, implications and outlook 20
4.1 Multisource remote sensing approaches for soil, crop and land-surface monitoring 20
4.2 Methodological limitations and sources of uncertainty 22
4.3 Practical implications and future outlook 23
5 Conclusion 26
6 References 28

List of original publications

This thesis is based on the following publications:

I **Mahmud, A.**, Luotamo, M., Karhu, K., Pellikka, P., Tuure, J., & Heiskanen, J. (2024). Comparison of field and imaging spectroscopy to optimize soil organic carbon and nitrogen estimation in field laboratory conditions. CATENA, 243, 108180.

II **Mahmud, A.**, Hoque, A., Tuure, J., Alakukku, L., Mäkelä, P. S. A., Wachiye, S., Mjomba, M., Pellikka, P. K. E., & Heiskanen, J. (2026). Integrating field camera imagery for monitoring maize phenology, biophysical traits, and agroclimatic factors in smallholder farms. Computers and Electronics in Agriculture, 240, 111161.

III **Mahmud, A.**, Tuure, J., Luo, Z., Mjomba, M., Pellikka, P. K. E., & Heiskanen, J. (2026). Multiscale Analysis of Vegetation Cover and Land Surface Temperature in Kenyan Smallholder Farms. Submitted.

The publications are referred to in the text by their roman numerals.

Author contribution

Contributions	I	II	III
Conceptualization	AM, JH	AM, JH	AM, JH
Resources & Investigation	JH	JT, SW, MM, PP, JH, LA, PM	JH, MM
Methodology	AM	AM, AH	AM
Software	AM	AM	AM
Data curation	AM, ML	AM, AH	AM
Formal analysis	AM	AM, AH	AM
Validation	AM	AM	AM
Visualization	AM, ML	AM	AM
Manuscript writing	AM	AM, AH	AM
Review and editing	JH, JT, KK, ML, PP	LA, PM, SW, PP, JH, JT	AM, JT, ZL, PP, JH

AM = Ashfak Mahmud, AH = Atikul Hoque, JH = Janne Heiskanen, JT = Juuso Tuure, KK = Kristiina Karhu, LA = Laura Alakukku, ML = Markku Luotamo, MM = Mwadime Mjomba, PM = Pirjo Mäkelä, PP = Petri Pellikka, SW = Sheila Wachiye, ZL = Zhaozhi Luo

List of figures

Figure 1: Study area map showing sampling locations and study sites of three articles… 7
Figure 2: Comparison between field-observed and extracted phenological dates using (a) inter-site and (b) within-site leave-one-out cross-validation (LOOCV). The grey dashed lines indicate a ±15-day range. 16
Figure 3: RF model performance for estimating FVC from PlanetScope (3 m), Sentinel-2 (10 m), and Landsat 8/9 (30 m) imagery using UAV orthomosaic-derived reference FVC. 17
Figure 4: Overview of the integrated remote sensing and proximal sensing workflow for monitoring soil, crop and land surface processes in smallholder cropping systems.. 21

List of tables

Table 1: Model performance metrics for SOC prediction from field spectroradiometer (FS) and imaging spectrometer (IS) using PLSR, LASSO, and GPR across ranges of wavelengths bands..... 14
Table 2: Model performance metrics for SN prediction from field spectroradiometer (FS) and imaging spectrometer (IS) using PLSR, LASSO, and GPR across ranges of wavelengths bands..... 15
Table 3: Pearson correlation coefficients between field camera-derived Green Chromatic Coordinate (GCC) and maize biophysical variables. 16
Table 4: Random Forest vegetation classification performance at the Kishenyi and Maktau sites evaluated with precision, recall, and F1-score. 17
Table 5: Summary of the relationships between FVC and LST at UAV and satellite scales across spatial scales, sites, years, and agroecological zones. 18

List of abbreviations

AEZ	Agroecological zone
BBCH	Biologische Bundesanstalt, Bundessortenamt und Chemische Industrie
DN	Digital number
ExG	Excess Green
FS	Field spectroradiometer
FVC	Fractional vegetation cover
FWR	Full wavelength range
GCC	Green chromatic coordinate
GEE	Google Earth Engine
GNSS	Global Navigation Satellite System
GPR	Gaussian process regression
IS	Imaging spectrometer
LAI	Leaf area index
LASSO	Least absolute shrinkage and selection operator
LH	Lower Highland
LM	Lower Midland
LOOCV	Leave-one-out cross-validation
LST	Land surface temperature
NDSI	Normalized difference spectral index
PLSR	Partial least squares regression
RA	Regenerative agriculture
RF	Random Forest
RMSE	Root mean square error
ROI	Region of interest
RPD	Ratio of performance to deviation
RPIQ	Ratio of performance to interquartile distance
RSI	Ratio spectral index
SN	Soil nitrogen
SNV	Standard normal variate
SOC	Soil organic carbon
SWIR	Shortwave infrared
UAV	Unmanned aerial vehicle
UM	Upper Midland
VI	Vegetation index
VNIR	Visible–near infrared

1 Introduction

1.1 Smallholder cropping systems and regenerative agriculture

Smallholder cropping systems are fundamental to food production and rural livelihoods, especially in sub-Saharan Africa, where agriculture is commonly organized in small, fragmented plots managed under diverse cropping practices and strong rainfall dependence (Ricciardi et al., 2018). In southeastern Kenya, these systems occur across marked agroecological gradients, from dry lowlands to wetter highlands, and are characterized by substantial variation in soils, land use, vegetation, and management intensity over short distances (Autio et al., 2021; Pellikka et al., 2013). On one hand, diversity in cropping systems can support adaptation; on the other, smallholder farmers often face soil degradation, nutrient depletion, climatic stress, and limited access to timely monitoring tools and external inputs.

Regenerative agriculture (RA) has gained increasing attention as a framework for improving the ecological sustainability and long-term resilience of these systems. Rather than focusing only on short-term yield maximization, RA emphasizes the restoration of soil health, enhancement of nutrient cycling, improvement of water retention, support for biodiversity, and maintenance of productive capacity through management interventions (Khangura et al., 2023; Rhodes, 2017). Common RA practices include reduced tillage, cover cropping, crop rotation, intercropping, and the use of organic amendments or nitrogen-fixing crops (Abdalla et al., 2019; Poeplau & Don, 2015). These practices are especially relevant in smallholder contexts because they can improve soil organic matter, reduce dependence on synthetic inputs, and strengthen resilience to climatic variability and environmental stress (Prescott et al., 2021).

Smallholder cropping systems should be understood as integrated biophysical systems in which soil condition, crop development, and land-surface processes are closely interconnected. Soil properties shape water and nutrient availability, crop growth reflects plant responses to environmental conditions and management, and land-surface characteristics such as vegetation cover and surface temperature indicate broader patterns of canopy development, soil exposure, and surface energy

exchange. In smallholder landscapes, these processes vary markedly across short distances due to differences in soils, topography, climate, land use, and management practices.

1.2 The need for scalable monitoring of soil, crop, and land-surface processes

The effectiveness of regenerative agriculture depends not only on management choices but also on the ability to monitor how soil, crops, and land-surface conditions respond over space and time. This need is especially important in smallholder landscapes, where fragmented fields, mixed cropping, and strong agroecological contrasts create rapid changes in biophysical and biochemical states within short distances. Soil properties such as organic carbon and nitrogen vary substantially at intra-field scale, crop development responds dynamically to weather, soil moisture, and management, and vegetation cover and surface temperature fluctuate with canopy growth, soil exposure, and moisture availability (Gao et al., 2017; He et al., 2021; Jandl et al., 2014). Reliable agricultural assessment therefore requires monitoring approaches that can capture both fine-scale variability and broader landscape patterns.

Conventional monitoring methods provide valuable information, but they are often resource-intensive or difficult to apply at broader scale. Laboratory analysis remains a reliable approach for measuring soil organic carbon (SOC) and soil nitrogen (SN), yet it is costly, time-consuming, and often difficult to access in remote areas or when large numbers of samples are involved (Conant et al., 2011; Sinfield et al., 2010; Tan et al., 2022). Likewise, ground-based crop growth observations can provide precise information on crop phenological, biophysical, and agroclimatic dynamics, but they are labor-intensive, spatially limited, and exposed to observer bias (Lobell et al., 2013; Mulla, 2013). In situ observations of land surface processes also require substantial field effort and may capture vegetation-thermal dynamics only at selected points rather than across the full heterogeneity of the landscape (He et al., 2021; Riihimäki et al., 2019). These limitations make it difficult to build consistent monitoring systems for smallholder agriculture using conventional methods alone.

Monitoring these dimensions together is especially important in heterogeneous smallholder systems, where soil condition, crop growth, vegetation cover, and thermal dynamics are closely interconnected and vary across fragmented fields, seasons, and agroecological zones. Field-based methods are necessary to capture fine-scale spatial variation, but broader spatial coverage is needed to identify patterns at landscape-level, while frequent observations are required to detect short-term changes driven by agroclimatic variability and management practices.

These requirements highlight the need for integrated monitoring approaches that combine local accuracy with repeated observations and wider spatial coverage, thereby explaining the growing importance of more scalable agricultural monitoring.

1.3 Remote sensing as a tool for agricultural monitoring

Remote sensing can be defined as the acquisition of information about the Earth's surface using sensors mounted on airborne or spaceborne platforms, based on the detection of electromagnetic radiation that is reflected, emitted, or returned from surface features (DeFries, 2013). Remote sensing has become an essential tool for agricultural monitoring because it enables repeated, non-destructive, and spatially explicit observation of biophysical processes that are otherwise difficult to assess consistently with conventional field methods alone (Weiss et al., 2020). Its value is evident in smallholder cropping systems, where fragmented fields, mixed cropping, and strong environmental heterogeneity make monitoring labor-intensive and difficult to scale. Across agricultural applications, remote sensing supports the observation of soil condition, crop development, vegetation status, and land-surface thermal behavior through measurements acquired at different spatial and temporal resolutions. In this way, it offers an important means of complementing field observations by extending monitoring from individual plots to farms, landscapes, and agroecological gradients (Angelopoulou et al., 2019; Gao et al., 2017; Li et al., 2023).

For soil monitoring, remote sensing provides alternatives and complements to conventional laboratory analysis, particularly through proximal and imaging spectroscopy in the visible, near-infrared, and shortwave-infrared spectral domains. These approaches exploit the relationship between soil reflectance and soil constituents, allowing the estimation of properties such as soil organic carbon and soil nitrogen with increasing accuracy when combined with multivariate modelling and machine learning methods (Angelopoulou et al., 2019; Ben-Dor & Banin, 1995; Stenberg et al., 2010). Their practical significance is considerable in agricultural contexts where laboratory access is limited, sample numbers are large, or rapid assessment is required. By reducing dependence on time-consuming chemical analyses, proximal sensing approaches improve the feasibility of monitoring soil condition in resource-constrained environments and strengthen the operational basis for monitoring regenerative management outcomes (Conant et al., 2011; Sinfield et al., 2010; Tan & Kuebbing, 2023).

In crop monitoring, remote sensing is especially valuable for tracking phenology and related biophysical changes and agroclimatic responses through time. Satellite image time series have greatly expanded the capacity to monitor seasonal crop

dynamics over broad areas, while near-surface systems such as field cameras provide high-frequency observations at plot scale and can capture progressive changes in canopy greenness, plant development, and agroclimatic responses with greater temporal detail (Diao et al., 2021; Diao & Li, 2022; Richardson et al., 2009). Such observations are important because crop growth stages strongly influence management needs, productivity, and sensitivity to environmental stress. In smallholder systems, however, the performance of satellite-based crop monitoring may be constrained by cloud cover, mixed pixels, and insufficient spatial resolution for very small fields, which has increased interest in combining satellite observations with near-surface monitoring approaches that offer finer spatial and temporal detail (Feng et al., 2024; Mulla, 2013; Vrieling et al., 2018).

Remote sensing is equally important for monitoring land-surface processes, particularly vegetation cover and land surface temperature. Fractional vegetation cover provides information on canopy development, soil exposure, evapotranspiration, and land degradation, whereas land surface temperature reflects land–atmosphere energy exchange, moisture conditions, and the thermal effects of vegetation cover (He et al., 2021; Kustas & Anderson, 2009; Li et al., 2013). UAV and satellite observations are especially valuable in this regard because they allow these variables to be examined across scales. Monitoring with UAVs can resolve field-level heterogeneity at centimeter resolution, while satellite systems such as PlanetScope, Sentinel-2, and Landsat extend analysis to broader regional patterns. Taken together, these capabilities make remote sensing particularly well suited to agricultural monitoring in heterogeneous smallholder landscapes, where understanding both fine-scale spatial variation and broader-scale variability is essential.

1.4 Research gaps and objectives

Despite major advances in agricultural monitoring, important limitations remain in the assessment of smallholder cropping systems. The central research gap, therefore, lies in the absence of an integrated and scalable framework that connects soil, crop, and land-surface processes across observation platforms and spatial scales. This gap is particularly significant in smallholder systems, where strong intra-field variability, fragmented field structure, and agroecological contrasts complicate both measurement and interpretation. Addressing this gap requires approaches that can combine detailed local measurements with broader spatial coverage, while also accounting for agroecological variability and the methodological differences among proximal, near-surface, UAV, and satellite observations. Such integration is necessary for moving beyond isolated indicators toward a more complete understanding of agricultural system functioning in

smallholder landscapes. To respond to this need, this thesis addresses three complementary objectives that examine soil, crop, and land-surface monitoring using multisource remote sensing approaches.

Objective 1: To assess proximal spectroscopy for rapid estimation of soil organic carbon and nitrogen in smallholder agricultural environments.

Evaluated the performance of two proximal hyperspectral sensors, an imaging spectrometer and a point-based field spectroradiometer, for rapid soil properties determination under field-laboratory conditions. Different sensors, wavelength regions, and machine-learning regression models were compared to determine their ability to estimate soil organic carbon and soil nitrogen accurately and efficiently.

Objective 2: To evaluate near-surface field cameras for high-frequency monitoring of crop phenology, biophysical attributes, and agroclimatic responses in smallholder cropping systems across agroecological zones.

Examined the use of field camera imagery for continuous monitoring of maize development in smallholder farms. Evaluated the relationships between camera-derived greenness signals, crop biophysical traits, and agroclimatic factors, and assessed the ability of field camera derived greenness time series to detect key phenological stages across different agroecological zones.

Objective 3: To develop a multisource remote sensing framework for estimating fractional vegetation cover and its relationship with land surface temperature across UAV and satellite scales in fragmented smallholder farms across agroecological zones.

Developed a multiscale remote sensing approach combining field, UAV, and satellite observations to estimate fractional vegetation cover. Examined how vegetation cover was related to land surface temperature across sites, years, and agroecological zones, thereby improving understanding of cross-scale vegetation–thermal dynamics in heterogeneous smallholder agricultural landscapes.

2 Materials and methods

2.1 Study area and agroecological setting

The study was conducted in Kenya, with field sites spanning both the central Kenyan highlands and the lowlands of southeastern Kenya. Taken together, the three articles cover environments that range from relatively cool and humid highland conditions to warmer and drier lowland settings, thereby providing a suitable basis for examining soil, crop, vegetation, and thermal processes under contrasting smallholder agricultural conditions. A major part of the work was situated in Taita Taveta County, where the landscape is characterized by dry lowland plains and more elevated highland areas with heterogeneous land cover, strong altitudinal variation, and bimodal rainfall pattern. Across this gradient, differences in elevation, rainfall regime, soil type, and land use create substantial environmental variability, which is central to the agroecological framing of the thesis.

Article I focused on the wider Taita Hills region in Taita Taveta County, southeastern Kenya (Figure 1). The study area extended along a lowland-to-highland transect of approximately 30 km, from the town of Mwatate at about 800 m a.s.l. to the montane environment of Vuria mountain at about 2000 m a.s.l. More broadly, the region was described as consisting of dry lowland plains at approximately 500–1000 m a.s.l. and highlands reaching about 2200 m a.s.l (Pellikka et al., 2023). Taita Hills contains nine agroecological zones (AEZs), and soil conditions vary markedly across these zones and with altitude (Jaetzold et al., 2010). The sampled agricultural environments included cropland, sisal plantation, agroforestry, and shrubland, which together captured a wide range of land-cover and soil-condition variability relevant to soil organic carbon and soil nitrogen assessment.

Article II covered three regenerative agriculture experimental sites in Kenya: Kabete, Kishenyi, and Maktau (Figure 1). Kabete is located at the University of Nairobi campus in the Kenyan highlands at 1900 m a.s.l., whereas Kishenyi and Maktau are located in Taita Taveta County in eastern Kenya at 1550 m and 1060 m a.s.l., respectively. These three sites represented distinct agroecological settings, with Kabete classified as Upper Midland Zone 2 (UM2), Kishenyi as Lower

Highland Zone 2 (LH2), and Maktau as Lower Midland Zone 5 (LM5). According to the World Reference Base for Soil Resources, dominant soils also differed among the sites, being Humic Nitisols in Kabete, Chromic Acrisols in Kishenyi, and Rhodic Ferralsols in Maktau (Jaetzold et al., 2010; Jaetzold & Schmidt, 1983). All three sites had contrasting environmental characteristics which made these sites appropriate for evaluating crop phenology, biophysical variability and agroclimatic responses across agroecological zones.

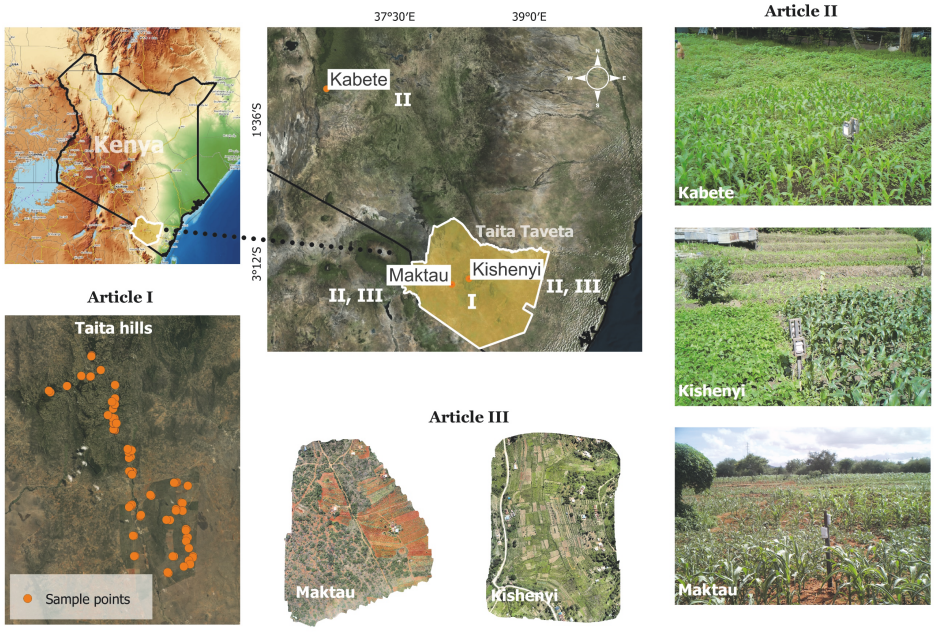

Figure 1: Study area map showing sampling locations and study sites of three articles.

Article III also focused on Kishenyi and Maktau sites in Taita Taveta County (Figure 1). In this study, Kishenyi represented a highland small-scale vegetable cultivation area at 1550 m a.s.l., whereas Maktau represented a warmer and lowland maize-dominated agricultural landscape at 1060 m a.s.l. The study landscapes extend across several AEZs, including Lower Highland Zone 2 (LH2), Upper Midland Zones 3 and 4 (UM3 and UM4), and Lower Midland Zones 4, 5, and 6 (LM4, LM5, and LM6; Jaetzold et al., 2010). These two sites therefore provided a suitable basis for examining vegetation cover and land surface temperature across scales under contrasting thermal and moisture conditions. Although Article III used Kishenyi and Maktau as the main observation sites, the analysis is framed within the wider agroecological and landscape gradient of Taita Hills and Taita Taveta County.

2.2 Overview of datasets and sensing platforms

The datasets associated with Articles I and II have been deposited in the Zenodo research data repository and are openly available as Mahmud et al. (2026a) and Mahmud et al. (2026b), respectively.

2.2.1 Agroclimatic datasets

The agroclimatic datasets were primarily used in Article **II** and Article **III**, which focused on regenerative agriculture experimental sites in Kabete, Kishenyi, and Maktau. At all three sites, weather stations were installed close to the experimental plots for continuous monitoring of precipitation, soil volumetric water content, relative humidity and air temperature.

2.2.2 Biophysical datasets

The biophysical datasets utilized mainly in Article **II** consisted of repeated field measurements that were collected to characterize maize growth and development under contrasting agroecological conditions at Kabete, Kishenyi, and Maktau. These measurements were conducted biweekly, starting when plants had developed two leaves and continuing until senescence when the uppermost leaves began to lose greenness. For each plot, ten plants were selected and marked for repeated observations, while border plants were excluded to reduce edge effects. Measurements were generally taken in the morning to improve consistency and minimize short-term environmental variation.

The crop biophysical variables measured in Article **II** were plant height, leaf chlorophyll content, stomatal conductance, and leaf area index (LAI). For each plot, the median of the ten plant-level measurements was used in subsequent analysis. In addition to the continuous biophysical measurements, phenological stage observations were recorded in Article **II** using the BBCH scale, with the timing of a stage defined as the point when 50% of the plants in a plot had reached that stage.

2.2.3 Proximal hyperspectral datasets

Two proximal hyperspectral sensors were used in Article **I**, representing two complementary forms of proximal hyperspectral sensing: point-based full-range spectroscopy and image-based VNIR hyperspectral imaging. The first was an SVC HR-1024i field spectroradiometer with 1024 spectral bands covering 350–2500 nm, equipped with a Leaf-Clip Reflectance-Probe and internal tungsten halogen lamp for contact-based reflectance measurements. The second sensor was a Specim

IQ imaging spectrometer, which captured 204 bands in the 400–1000 nm range at 7 nm spectral resolution.

2.2.4 Field camera images

Field camera images from two sensors were employed in Articles **II** and **III**, but the two imaging sources served different purposes. In Article **II**, six Bushnell Trophy Cam E3 trail cameras were installed in February 2023 at the three regenerative agriculture sites: two cameras in Kabete, two in Kishenyi, and two in Maktau. The cameras were mounted on metal poles at about 3 m height and programmed to capture four JPEG images per day, twice in the morning and twice in the afternoon. Across the two growing seasons, 32,976 images were collected, of which 8,244 morning images were selected for analysis after visual quality control.

In Article **III**, digital field photographs were collected using a Nikon D5000 camera equipped with an 18 mm lens. The photographs were taken in nadir orientation from a monopod to capture the canopy directly above the sampling point over an area of 0.5 m². A total of 185 field photographs were acquired, including 96 from Maktau and 89 from Kishenyi, and the center of each image footprint was georeferenced with a Trimble GeoXH 6000 GNSS receiver. Unlike the Bushnell time series, these digital photographs were used as field reference data for estimating and validating fractional vegetation cover.

2.2.5 UAV images

UAV datasets used in Article **III** consisted of RGB and thermal imagery collected during the 2024 and 2025 growing seasons at Kishenyi and Maktau. The flights were carried out under clear, sunny conditions using a DJI Matrice 300 RTK platform equipped with a DJI Zenmuse P1 RGB camera and a DJI H20T thermal camera. The UAV campaigns were conducted on 4 and 5 June 2024 and on 22 and 23 May 2025. UAV flown at 80 m above ground level and forward overlap of 80% and 70% side overlap. The RGB imagery had a ground sampling distance of 2.2 cm, and the thermal imagery 7.3 cm. Thermal images were first converted from radiometric JPEG to calibrated TIFF using a custom R workflow integrating the DJI Thermal SDK, with radiometric correction based on emissivity, relative humidity, target distance, and air temperature. Five ground control points were established at each site for accurate georeferencing, and the UAV data were processed photogrammetrically in Pix4Dmapper to produce georeferenced RGB and thermal orthomosaics. The photogrammetric workflow consisted of image alignment, automated keypoint extraction and matching, GCP markings, and generating dense point clouds.

2.2.6 Satellite images

Satellite datasets were used in Article **III** to extend vegetation-cover and land-surface temperature analysis beyond UAV scale. The imagery included PlanetScope (PS, 3 m), Sentinel-2 (S2, 10 m), Landsat 8 (L8, 30 m), and Landsat 9 (L9, 30 m) acquisitions acquired within approximately 5–9 days of the UAV flights, while in 2025, Landsat 9 was acquired within 2–3 days and PS and S2 approximately three weeks after the UAV campaigns. PS images were acquired for 12 June 2024 and 13 June 2025, S2 for 13 June 2024 and 13 June 2025, L8 for 30 May 2024 and L9 for 25 May 2025.

The Landsat data were obtained as Collection 2 Level-2 atmospherically corrected products through Google Earth Engine (GEE) and included visible, near-infrared, shortwave infrared, and thermal bands. Digital numbers (DN) from optical bands were converted to physical surface reflectance using the standard scaling factor (DN×0.0000275−0.2). Pixels affected by clouds, cloud shadows, and water were excluded based on the QA_PIXEL quality mask (USGS, 2019, 2022). For land surface temperature analysis, the ST_B10 band was used as the LST variable, as it provides atmospherically corrected surface temperature at 30 m spatial resolution. DN values were converted to temperature in Kelvin using the scale factor and offset, LST_K = DN×0.00341802+149.0, and were then converted to degrees Celsius by subtracting 273.15 (USGS, 2024). Sentinel-2 surface reflectance imagery was also accessed via GEE, with cloud screening performed using the Cloud Score+ quality bands. PlanetScope Super Dove Ortho Scene Surface Reflectance imagery was acquired from Planet Explorer. Images were automatically harmonized to Sentinel-2 equivalents and filtered using the usable data mask to retain only clear pixels.

2.3 Soil spectroscopy for organic carbon and nitrogen determination

In Article I**,** a soil spectroscopy workflow in field laboratory conditions was designed to support rapid assessment of SOC and SN in agricultural environments. The analysis was based on 157 soil samples collected from agricultural sites in Taita Hills, Kenya. Reference SOC and SN contents were first determined using a Leco CN828 dry oxidation analyzer, after which the air-dried soil samples were measured spectrally using protocols developed for field-laboratory conditions (Pellikka et al., 2023). The overall purpose of the study was to compare sensor types, wavelength ranges, and modelling approaches for estimating SOC and SN from soil spectra.

Two proximal hyperspectral sensors were used: a point-based full-range spectroradiometer and an image-based hyperspectral imaging spectrometer. The point-based measurements were acquired with an SVC HR-1024i field spectroradiometer, which captured 1024 bands in the 350–2500 nm range and was operated with a Leaf-Clip Reflectance Probe (LC-RP PRO; (SVC, 2020). The imaging measurements were acquired with a Specim IQ imaging spectrometer which recorded 204 spectral bands in the 400–1000 nm range. Each soil sample was placed in a petri dish, and each sample was measured three times, with white reference measurements taken between measurements.

After spectral acquisition, several preprocessing steps were applied to improve spectral quality and comparability. For the SVC HR-1024i data, noisy wavelengths at 350–399 nm and 2400–2500 nm were removed, the overlapping detector regions around 990 nm and 1900 nm were matched and spliced to reduce inter-sensor inconsistency (Meireles et al., 2023), and the three replicate measurements per sample were averaged. For the Specim IQ data, the soil-only region was extracted from each hyperspectral image using a HoughCircles-based segmentation approach, after which 22 noisy bands were removed and 182 bands (440–972 nm) were retained. Mean pixel spectra were then calculated for each sample (Pellikka et al., 2023). Finally, all spectra from both instruments were corrected using standard normal variate (SNV) transformation to minimize scattering effects and normalize spectral variation prior to modelling (Barnes et al., 1989).

For spectral modelling, three regression methods were evaluated: partial least squares regression (PLSR; (Martens & Naes, 1992), Gaussian process regression (GPR; (Rasmussen, 2004), and least absolute shrinkage and selection operator (LASSO; (Tibshirani, 1996). The field spectroradiometer data were assessed over the full wavelength range (FWR; 400–2400 nm), visible–near-infrared range (VNIR; 400–1000 nm) and shortwave infrared range (SWIR; 1000-2400 nm). Model performance was assessed using 10-fold cross-validation, and accuracy was compared using the coefficient of determination (R^2) and root mean square error (RMSE), ratio of performance to deviation (RPD) and ratio of performance to inter-quartile distance (RPIQ).

2.4 Monitoring crop phenology, biophysical traits, and agroclimatic variability using field cameras

Article **II** focused on the use of field camera imagery to monitor maize phenology, crop biophysical traits, and agroclimatic variability across agroecological zones. For each camera, a fixed region of interest (ROI) was defined to isolate the target plot while excluding sky background and vegetation from neighbouring plots. The green chromatic coordinate (GCC) was derived from the red, green, and blue channels within the ROI (Richardson et al., 2007). The mean GCC value of each image was used to construct a daily time series for each monitored plot. To reduce short-term noise unrelated to crop development, the GCC time series were smoothed using a second-order Savitzky–Golay filter (Savitzky & Golay, 1964).

The GCC time series were analysed in relation to field-measured crop biophysical variables and agroclimatic observations from Kabete, Kishenyi and Maktau sites. Plant height, leaf chlorophyll content, stomatal conductance, and LAI were used as biophysical variables, and their median values were derived at plot level. GCC was also compared with rainfall and soil moisture observations obtained from the three weather stations. The relationship between greenness and agroclimatic conditions was evaluated using daily-scale Pearson lag correlation, which made it possible to assess delayed crop responses to rainfall and soil-moisture variability across sites.

Phenological stages observed in BBCH (Biologische Bundesanstalt, Bundessortenamt und CHemical Industry) scale were used as reference data for evaluating phenology retrieval from field imagery. Six key maize phenological stages including emergence, stem elongation, tasseling, kernel development, ripening, and senescence were considered. These stages were extracted from the GCC time series using a relative amplitude-based threshold method via a within-site and inter-site validation approach. In addition, the threshold-based retrieval was compared against established curve-fitting baseline methods, derivative-based method (DER, Filippa et al., 2016), GU-method (Gu et al., 2009) and Klosterman-method (Klosterman et al., 2014).

2.5 Multiscale analysis of fractional vegetation cover and land surface temperature

Article **III** focused on developing a multiscale framework for estimating fractional vegetation cover (FVC) and analysing its relationship with land surface temperature (LST) across field, UAV, and satellite scales. First, Excess Green (ExG) index was calculated from field photographs, after which vegetation was extracted through Otsu thresholding algorithm (Otsu, 1979). For the UAV orthomosaics, vegetation was classified from the RGB imagery using a Random Forest model in order to separate vegetation from non-vegetation at very high spatial resolution (2.2 cm).

The classified vegetation masks were subsequently used to derive reference FVC at 3 m, 10 m, and 30 m spatial resolutions, corresponding to the pixel grids of PlanetScope, Sentinel-2, and Landsat 8/9, respectively. These aggregated FVC values were then used as reference data for upscaling FVC at satellite scale. For each satellite sensor, a RF regressor (Breiman, 2001) was trained using spectral bands, vegetation indices (VI) and all pairwise band combinations used to derive ratio spectral indices (RSI) and normalized difference spectral indices (NDSI) to train and cross-validate (5 fold) FVC at the corresponding spatial resolution. The trained models were then used to estimate FVC from satellite imagery, resulting in continuous maps at 3 m, 10 m, and 30 m spatial resolution.

The relationship between FVC and LST was analysed jointly across UAV and satellite scales, sites, and AEZs. For the UAV analysis, co-registered FVC and LST were aggregated to 3 m, 10 m, and 30 m grids for Kishenyi and Maktau in 2024 and 2025. Within each grid cell, median LST was used to reduce the influence of extreme thermal pixels such as bare-soil hotspots, shadows, and canopy gaps. At the satellite scale, relationships between Landsat 8/9-derived FVC and LST were analysed across six AEZs.

3 Results and discussion

3.1 Estimation of soil organic carbon and nitrogen

In Article **I**, soil spectroscopy analysis showed that SOC was estimated more accurately than SN, and FS performed better than the IS. The best model for SOC achieved R^2 = 0.83 with RMSE = 0.36%, while the best SN model reached R^2 = 0.70 with RMSE = 0.07% (Table 1 and Table 2). The performance of the SOC prediction in the FWR showed good correspondence with previous studies (Chen et al., 2019; Lazaar et al., 2020; Miloš & Bensa, 2017; Morellos et al., 2016; Wijewardane et al., 2016). Although our SN models performed less accurately than in He et al. (2005), Vibhute et al. (2020), and Xiao & He, (2019), they showed good agreement with Erler et al. (2020), Madari et al. (2006), and Martin et al. (2002).

Table 1: Model performance metrics for SOC prediction from field spectroradiometer (FS) and imaging spectrometer (IS) using PLSR, LASSO, and GPR across ranges of wavelength ranges.

Sensor	Model	Spectral range	R^2	RMSE	RPD	RPIQ
FS	PLSR	VNIR	0.56	0.59	1.52	2.32
FS	LASSO	VNIR	0.61	0.55	1.61	2.46
FS	GPR	VNIR	0.52	0.61	1.45	2.23
FS	PLSR	FWR	0.82	0.38	2.35	3.61
FS	LASSO	FWR	0.83	0.37	2.43	3.72
FS	GPR	FWR	0.82	0.37	2.38	3.65
FS	PLSR	SWIR	0.83	0.37	2.44	3.74
FS	LASSO	SWIR	0.82	0.37	2.39	3.66
FS	GPR	SWIR	0.83	0.36	2.47	3.78
IS	PLSR	VNIR	0.62	0.55	1.63	2.50
IS	LASSO	VNIR	0.67	0.51	1.75	2.68
IS	GPR	VNIR	0.68	0.50	1.78	2.73

VNIR = visible-near infrared, FWR = full wavelength range, SWIR = shortwave infrared, RMSE = root mean square error, RPD = ratio of performance to deviation, RPIQ = ratio of performance to inter-quartile distance.

In addition, SOC and SN models using the full wavelength range or particularly the SWIR region clearly outperformed those based only on the VNIR range. These results are consistent with earlier studies showing that SOC and SN estimation generally benefits from SWIR information because this region contains stronger absorption features related to organic and mineral soil constituents (Angelopoulou et al., 2019; Stenberg et al., 2010). The lower accuracy for SN than for SOC also

agrees with previous findings that nitrogen has no strong direct spectral response and can therefore be estimated only indirectly, from spectral features of covarying soil constituents such as organic matter (Stenberg et al., 2010; Viscarra Rossel et al., 2006). Overall, the results indicate that broad-range proximal hyperspectral sensing is a promising and operationally efficient approach for rapid soil properties assessment in agricultural environments.

Table 2: Model performance metrics for SN prediction from field spectroradiometer (FS) and imaging spectrometer (IS) using PLSR, LASSO, and GPR across ranges of wavelengths bands.

Sensor	Model	Spectral range	R^2	RMSE	RPD	RPIQ
FS	PLSR	VNIR	0.39	0.10	1.28	1.98
FS	LASSO	VNIR	0.42	0.10	1.32	2.06
FS	GPR	VNIR	0.49	0.09	1.40	2.24
FS	PLSR	FWR	0.64	0.08	1.66	2.66
FS	LASSO	FWR	0.60	0.08	1.58	2.53
FS	GPR	FWR	0.70	0.07	1.84	2.95
FS	PLSR	SWIR	0.58	0.09	1.55	2.48
FS	LASSO	SWIR	0.59	0.08	1.57	2.51
FS	GPR	SWIR	0.67	0.08	1.73	2.77
IS	PLSR	VNIR	0.42	0.10	1.31	2.10
IS	LASSO	VNIR	0.42	0.10	1.32	2.10
IS	GPR	VNIR	0.53	0.09	1.46	2.34

VNIR = visible-near infrared, FWR = full wavelength range, SWIR = shortwave infrared, RMSE = root mean square error, RPD = ratio of performance to deviation, RPIQ = ratio of performance to inter-quartile distance.

3.2 Monitoring of crop phenology, biophysical and agroclimatic variables

In Article **II**, GCC time series from field camera captured variations in agroclimatic factors (rainfall and soil moisture) and biophysical attributes (leaf area index, crop height, chlorophyll content, and stomatal conductance) across AEZs. GCC showed positive relationships (r = 0.48 - 0.79) with key biophysical variables (Table 3), especially plant height, chlorophyll content, and leaf area index, confirming that the image-derived greenness signal reflected important structural and physiological changes in maize canopies (Aasen et al., 2020; Liu et al., 2022; Liu et al., 2015). Daily-scale Pearson lag correlation between GCC and agroclimatic factors confirmed that crops in the drier site responded more rapidly to agroclimatic variability, with lagged responses of about 32 days to rainfall and 14 days to soil moisture. This indicates a stronger short-term sensitivity of canopy development under moisture-limited conditions, suggesting that drier and hotter ecosystems can exhibit rapid shifts in greenness following rainfall events, as previously observed in African drylands (Wei et al., 2019).

Table 3: Pearson correlation coefficients between field camera-derived Green Chromatic Coordinate (GCC) and maize biophysical variables.

Variable	Kabete	Kishenyi	Maktau
Plant Height	0.70**	0.69**	0.79**
Chlorophyll	0.48**	0.56**	0.75**
Stomatal Conductance	N/A	0.01	-0.06
LAI	0.62**	0.71**	0.55**

Correlations significant at $p < 0.01$ are indicated by double asterisk (**).

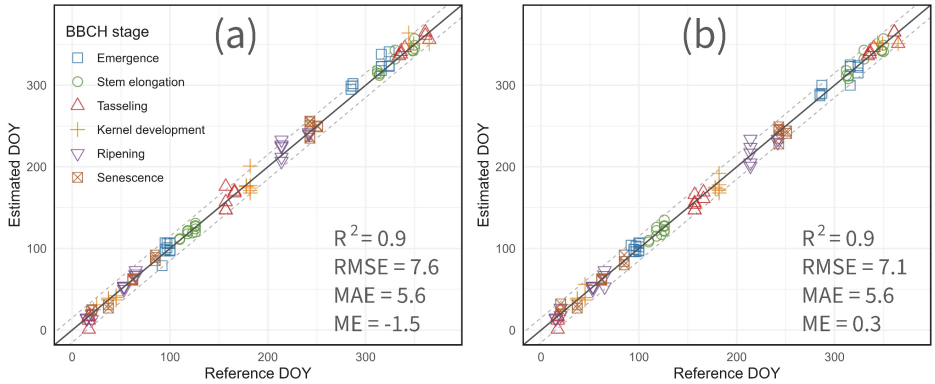

Figure 2: Comparison between field-observed and extracted phenological dates using (a) inter-site and (b) within-site leave-one-out cross-validation (LOOCV). The grey dashed lines indicate a ±15-day range.

Maize key phenological stages retrieval results demonstrated that field camera derived GCC effectively detected key phenological stages (emergence, stem elongation, tasseling, kernel development, ripening, and senescence) accurately, with R^2 of 0.90 and RMSE between 7.1 to 7.7 days in inter-site and within-site cross-validation (Figure 2). This accuracy is comparable to the results reported in several earlier near-surface and high-resolution remote sensing studies of crop phenology (Diao & Li, 2022; Guo et al., 2022; Liu et al., 2022). At the same time, the variation in retrieval accuracy among sites and growth stages supports the broader literature that phenological responses are modified by local agroclimatic conditions and may benefit from site-specific calibration (Guo et al., 2022; Hufkens et al., 2012). Thus, field cameras appear to provide a robust and low-cost tool for monitoring crop development in heterogeneous smallholder systems.

3.3 Multiscale analysis of fractional vegetation cover and land surface temperature

In Article **III**, FVC was estimated reliably from UAV imagery and then upscaled to satellite scale, although performance differed among sensors. At the UAV scale, vegetation classification with RF model was highly accurate, with precision, recall,

and F1-scores all above 0.96 (Table 4). These findings are in agreement with previous studies that have identified RF as a robust and dependable method for vegetation classification from UAV-based RGB orthomosaics, particularly in complex and heterogeneous agricultural environments (Al-Ali et al., 2020; Feng et al., 2015; Rose et al., 2023; Yang et al., 2023; Zhang et al., 2025). Validation against field photographs showed strong agreement with UAV-derived FVC (r = 0.84–0.85), indicating reliable estimation of vegetation cover under field conditions, although some scale-related bias remained at low and high FVC levels (Chen et al., 2024; Li et al., 2023).

Table 4: Random Forest vegetation classification performance at the Kishenyi and Maktau sites evaluated with precision, recall, and F1-score.

Site	Precision	Recall	F1
Kishenyi 2024	0.977	0.986	0.981
Kishenyi 2025	0.973	0.966	0.970
Maktau 2024	0.997	0.998	0.997
Maktau 2025	0.999	0.999	0.999

At the satellite scale, model performance improved from PlanetScope (r = 0.72, RMSE = 24.4%) to Sentinel-2 (r = 0.81, RMSE = 16.8%) and Landsat 8/9 (r = 0.82, RMSE = 13%) (Figure 3). The higher accuracy observed at coarser resolutions can be largely explained by spatial aggregation, which reduces local variance as pixel size increases (Woodcock & Strahler, 1987). In this context, our results suggest that aggregating UAV-derived FVC to satellite pixel size likely reduced very fine-scale heterogeneity and local noise, which would explain why Landsat and Sentinel-2 performed better than PlanetScope despite their coarser resolution.

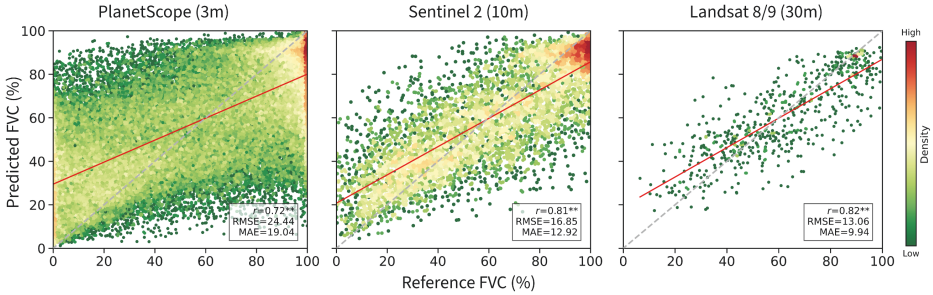

Figure 3: RF model performance for estimating FVC from PlanetScope (3 m), Sentinel-2 (10 m), and Landsat 8/9 (30 m) imagery using UAV orthomosaic-derived reference FVC. Point colors indicate density from low (dark green) to high (dark red). The dashed line shows the 1:1 relationship, while the solid red line represents the fitted linear regression. Statistically highly significant values ($p < 0.01$) are indicated by double asterisks (**).

Table 5: Summary of the relationships between FVC and LST at UAV and satellite scales across spatial scales, sites, years, and agroecological zones. The fitted slope (β_1) denotes the change in LST (°C) per one-percentage-point increase in FVC.

Sensor	Site / AEZ	Year	Spatial resolution	Correlation coefficient (r)	Fitted slope, β_1
UAV	Kishenyi	2024	3 m	-0.70	-0.16
UAV	Kishenyi	2024	10 m	-0.73	-0.18
UAV	Kishenyi	2024	30 m	-0.71	-0.19
UAV	Kishenyi	2025	3 m	-0.70	-0.16
UAV	Kishenyi	2025	10 m	-0.71	-0.17
UAV	Kishenyi	2025	30 m	-0.67	-0.17
UAV	Maktau	2024	3 m	-0.76	-0.18
UAV	Maktau	2024	10 m	-0.75	-0.21
UAV	Maktau	2024	30 m	-0.71	-0.27
UAV	Maktau	2025	3 m	-0.79	-0.19
UAV	Maktau	2025	10 m	-0.80	-0.19
UAV	Maktau	2025	30 m	-0.83	-0.19
Landsat 8	LH2	2024	30 m	-0.20	-0.08
Landsat 8	UM3	2024	30 m	-0.46	-0.16
Landsat 8	UM4	2024	30 m	-0.78	-0.31
Landsat 8	LM4	2024	30 m	-0.64	-0.19
Landsat 8	LM5	2024	30 m	-0.51	-0.10
Landsat 8	LM6	2024	30 m	-0.51	-0.09
Landsat 9	LH2	2025	30 m	-0.22	-0.10
Landsat 9	UM3	2025	30 m	-0.27	-0.09
Landsat 9	UM4	2025	30 m	-0.45	-0.16
Landsat 9	LM4	2025	30 m	-0.57	-0.26
Landsat 9	LM5	2025	30 m	-0.47	-0.16
Landsat 9	LM6	2025	30 m	-0.29	-0.07

A second key result was that the relationship between FVC and LST remained consistently negative across scales, indicating that higher vegetation cover was associated with lower surface temperature (Table 5). This negative relationship is widely reported in previous studies and is generally explained by the cooling effect of vegetation, which lowers sensible heat flux and reduces surface temperature through stomatal transpiration and shading of the soil surface (Carlson & Ripley, 1997; Sun & Kafatos, 2007; Weng et al., 2004). At the UAV scale, this relationship was stronger in Maktau ($r = -0.71$ to -0.83) than in Kishenyi ($r = -0.67$ to -0.73), suggesting a more pronounced cooling effect of vegetation in the warmer and drier site (Sandholt et al., 2002; Sun & Kafatos, 2007).

The strongest satellite-scale FVC–LST relationship was observed in UM4 in 2024 ($r = -0.78$), whereas much weaker relationships occurred in the cooler and wetter upper zones, such as LH2 ($r = -0.20$ to -0.22) and UM3 ($r = -0.46$ in 2024; $r = -0.27$ in 2025). This suggests that the cooling effect of vegetation was strongest under intermediate agroecological conditions, while in wetter upland areas other controls such as topography and other environmental factors (air temperature, rainfall, soil moisture, and humidity) likely reduced the explanatory power of FVC alone (Aalto et al., 2022; Abera et al., 2023; Fischer & Antoine, 1994; Sandholt et

al., 2002; Weng et al., 2004). The fitted slopes quantified the magnitude of this association. At the UAV scale, a one-percentage-point increase in FVC corresponded to a 0.16–0.27 °C reduction in LST, with steeper slopes at Maktau than at Kishenyi, whereas at the satellite scale the slopes ranged from −0.07 to −0.31 °C per percentage point across agroecological zones. Overall, the results support the conclusion that integrating field photographs, UAV imagery, and satellite observations provides an effective multiscale framework for analysing vegetation cover and thermal dynamics in fragmented smallholder systems.

4 Synthesis, implications and outlook

4.1 Multisource remote sensing approaches for soil, crop and land-surface monitoring

Taken together, the three articles showed that remote sensing can support integrated monitoring of soil properties, crop development, vegetation cover, and surface thermal dynamics in heterogeneous smallholder systems, but that the suitability of each sensing approach depends on the process being monitored and the scale of observation. A critical finding across the studies is that moving from ground-level to landscape-level sensing provides complementary insights into agricultural productivity and soil health. The main contribution of the thesis is therefore not only the evaluation of individual methods, but the demonstration of how these methods can be positioned within a practical multisource monitoring strategy for soil condition, crop development, and land-surface processes in heterogeneous smallholder landscapes (Figure 4a). Their usefulness therefore depends not only on technical performance, but also on the monitoring purpose, required spatial and temporal detail, and the intended user.

In Article **I**, proximal spectroscopy enabled estimation of SOC and SN, with the field spectroradiometer outperforming the imaging spectrometer, and the best results obtained when the full wavelength range, particularly the SWIR region was included. In practical terms, this approach is most valuable for remote places with limited laboratory access, where many soil samples need to be analyzed rapidly and consistently (Figure 4b). In Article **II**, field camera imagery proved useful not only for reliably tracking maize phenology, but also for capturing biophysical variation and agroclimatic responses. Such capability is especially important in smallholder cropping systems, where field fragmentation and small plot sizes limit the effectiveness of satellite imagery, while cloud cover further constrains optical observations. Field cameras address these limitations by providing continuous, plot-scale observations that can resolve subtle changes in canopy greenness, crop development, and short-term responses to environmental variability (Diao & Li, 2022; Lobell et al., 2003; Mulla, 2013; Vrieling et al., 2018). In Article **III**, combination of UAV and satellite data was ideal when the objective was to move

from detailed field-level characterization to broader landscape-scale vegetation and thermal dynamics monitoring. This demonstrates the practical value of multiscale monitoring for transferring reliable local observations into regional products, particularly where field measurements alone are spatially limited (Chen et al., 2024; Duan et al., 2016; Martínez Prentice et al., 2024).

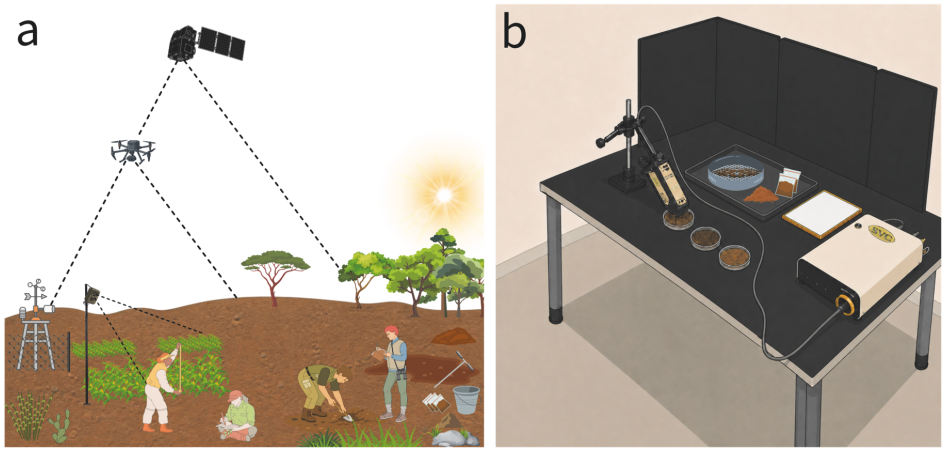

Figure 4: Overview of the integrated remote sensing and proximal sensing workflow for monitoring soil, crop and land surface processes in smallholder cropping systems. (a) Multisource data acquisition from satellite, UAV, field camera, weather station and in situ field observations for monitoring smallholder cropping system and (b) field collected soil spectral measurement with field spectroradiometer under controlled illumination conditions.

Methodologically, the thesis contributes in three ways. First, it demonstrates that field-laboratory proximal spectroscopy can support rapid estimation of SOC and SN in agricultural soils, thereby extending the practical relevance of soil spectroscopy for remote or infrastructure-limited settings, which has been highlighted as a key challenge in earlier work (Angelopoulou et al., 2019; Hong et al., 2018). Second, it shows that low-cost field cameras can provide high-frequency crop monitoring in smallholder farms, offering an alternative solution for tedious and costly in situ observations and challenges of coarser satellite observations, consistent with the growing role of near-surface remote sensing in phenology research (Diao & Li, 2022; Sonnentag et al., 2012; Vrieling et al., 2018). Third, it demonstrates the value of combining UAV and satellite data to analyse FVC and LST across scales, contributing to current efforts to address cross-sensor interoperability and scalability in agricultural remote sensing (Chen et al., 2024; Fawcett et al., 2020; Jiang et al., 2022).

4.2 Methodological limitations and sources of uncertainty

Despite these contributions, the thesis also has several methodological limitations that should be considered critically. In article **I**, spectral measurements were conducted under controlled field-laboratory conditions using air-dried and sieved soil samples. This improved spectral consistency, but it also means that the results may not transfer directly to in situ field conditions, where soil moisture, roughness, and illumination introduce additional variability. In addition, the comparison between the field spectroradiometer and the imaging spectrometer was not purely sensor-based, because the two instruments also differed in spectral range, particularly in the availability of SWIR information. Similar challenges of transferability and comparability have been raised in earlier spectroscopy literature (Nocita et al., 2015; Stenberg et al., 2010).

In Article **II,** certain maize phenological stages were difficult to identify using GCC alone because their visual expression was not always dominated by changes in green canopy cover. This is particularly relevant for transitioning to tasseling and kernel development without necessarily producing a clear greenness change. Field camera image-derived GCC was also affected by acquisition conditions, including illumination, image quality, and viewing angle. As the cameras were installed in an oblique position, the recorded canopy signal may include or be partially blocked by non-leaf plant components, which can introduce uncertainty in phenological interpretation (Vrieling et al., 2018). The use of low-cost RGB cameras further restricted the method, as these systems generally lack manual control over exposure and white balance and do not provide near-infrared information, limiting their usefulness for biochemical trait monitoring (Aasen et al., 2020; Zhao & Qu, 2024). In addition, differences among maize cultivars across agroecological zones may influence growth dynamics and the timing of phenological events. Relative threshold-based approaches may therefore require recalibration for different vegetation indices, crop types, cultivars, and environmental settings.

In Article **III** at the UAV level, the very fine spatial detail that supports field-scale analysis can also introduce uncertainty. In small and heterogeneous agricultural plots, shadowing, illumination differences, radiometric variation, and minor registration errors may alter the apparent vegetation signal and affect the comparison between UAV products and reference observations (Dare, 2005; Delavarpour et al., 2021; Lopatin et al., 2019; Riihimäki et al., 2019). Thermal estimates from UAV imagery also depend strongly on the emissivity values assigned to mixed surfaces, where exposed soil, crop canopy, and changing crop conditions may occur within short distances. Therefore, during LST retrieval, uniform emissivity value or average meteorological data input can introduce small bias LST

estimates (Heinemann et al., 2020). At the satellite level, the main limitation is scale mismatch. Coarser sensors such as Landsat may not fully capture within-field variability in fragmented smallholder landscapes, and even short acquisition differences between UAV and satellite images can introduce inconsistencies when management operations or irrigation rapidly change vegetation cover and surface temperature (Chen et al., 2020). Another limitation is that the satellite FVC models were trained and validated using UAV reference data from only two AEZs, while FVC was subsequently mapped and analysed across six AEZs. However, stratified group K-fold cross-validation was incorporated to reduce spatial autocorrelation and improve model generalization.

4.3 Practical implications and future outlook

The practical value of this thesis lies in showing that effective monitoring of smallholder farms through a combination of simple, inexpensive and reliable tools and approaches at the field-level and methods that enable repeated observations across larger areas. This is especially relevant in East Africa, where smallholders account for a large share of agricultural production and employment, yet productivity growth continues to be constrained by weak institutions, limited access to markets and credit, inadequate infrastructure, and restricted access to technology (Salami et al., 2010). In such settings, monitoring tools must be not only scientifically robust but also affordable, operationally feasible, and adaptable to fragmented landscapes and resource-constrained institutions.

Laboratory-based soil properties analysis to support soil health monitoring, although reliable, is often too costly, slow, or inaccessible for routine use in many agricultural regions, especially in remote areas (Angelopoulou et al., 2019; Conant et al., 2011). The findings in Article **I**, therefore, demonstrate the potential of soil spectroscopy in shared or centralized monitoring settings, such as research stations, extension-linked laboratories, or mobile diagnostic services, rather than as a farmer-level technology. In practical terms, this creates a realistic pathway for faster soil-health screening and more frequent assessment of key soil indicators relevant to regenerative agriculture and climate-smart agriculture (Autio et al., 2021).

In smallholder cropping systems, conventional field observations are often too sparse and labor-intensive to capture rapid changes in crop phenology, biophysical condition, and agroclimatic response, especially when neighboring plots differ in sowing date, management, or moisture availability. This creates an important monitoring gap between detailed but infrequent field visits and broader remote sensing products that may lack sufficient temporal or spatial resolution. Article **II** demonstrated that field cameras can provide a practical intermediate bridge

between field observation and broader remote sensing systems by offering continuous plot-scale monitoring of crop phenology, biophysical traits, and agroclimatic responses. Field cameras can serve not only as crop monitoring instruments, but also as low-cost validation and calibration tools that strengthen the interpretation of crop condition from broader earth observation products.

In fragmented smallholder landscapes, monitoring vegetation cover and land surface temperature is challenging because field conditions vary over short distances and seasons, while single-sensor approaches often fail to capture both fine-scale heterogeneity and broader spatial patterns. Satellite imagery alone may overlook local variation in small fields, whereas field-based observations are too limited to describe landscape-scale dynamics. In addition, differences in spatial resolution, sensor characteristics, and observation scale create uncertainty when linking field conditions to satellite-derived indicators, highlighting a persistent problem of scale mismatch in agricultural monitoring (Fawcett et al., 2020; Jiang et al., 2022; Li et al., 2023). Article **III** addressed these limitations by combining UAV and satellite observations to analyse critical land surface processes across scales. In this framework, UAV data were used for high-resolution local mapping, calibration, and validation, while satellite imagery provided wide-area coverage where direct field measurements are spatially limited.

When viewed together, the three articles suggest a practical architecture for smallholder farm monitoring. Soil spectroscopy can support targeted assessment of soil fertility and soil-health indicators; field cameras can provide continuous monitoring of crop development and phenological dynamics; and UAV–satellite integration can extend vegetation and thermal monitoring from field to landscape scale. This type of tiered monitoring system is particularly relevant for East African smallholder agriculture, where productivity gains are still urgently needed and where improved information can support better targeting of interventions, earlier detection of stress, and more evidence-based management decisions (Nakalembe et al., 2021; Salami et al., 2010).

Looking ahead, the future of smallholder farm monitoring should depend less on new sensor development alone and more on integration, cost-effectiveness, methodological simplicity, and scalability. Major opportunity already exists in the form of open-access and cloud-enabled agricultural monitoring platforms, but that uptake is often limited by gaps in technical capacity, baseline datasets, and institutional frameworks (Nakalembe et al., 2021). This suggests that future efforts should focus on linking research-grade methods with operational systems through better smallholder farm datasets, more consistent field-based reference observations, and stronger collaboration among researchers, extension services, and national monitoring agencies. From that perspective, the long-term value of

this thesis is not only in demonstrating the usefulness of individual methods, but also in showing how soil, crop, and land-surface monitoring can be connected within a broader and more operational vision of smallholder agricultural monitoring.

5 Conclusion

This thesis shows that monitoring smallholder agriculture cannot rely on a single variable, sensor, or scale of observation. In fragmented cropping systems, soil condition, crop development, vegetation cover, and surface thermal behaviour are tightly connected, yet each becomes visible only through different measurement strategies. By bringing together soil spectroscopy, field camera monitoring, and UAV–satellite analysis, the thesis develops a more coherent view of how remote sensing can move from isolated measurements toward an integrated understanding of smallholder farm condition.

In the first study, proximal spectroscopy offers a practical route for faster assessment of key soil indicators where laboratory access is limited. In the second study, field cameras fill the temporal gap between occasional field visits and coarser satellite observations by tracking crop development continuously at plot scale. In the third study, UAV and satellite data extend this perspective outward, making it possible to connect fine field-level assessment of vegetation cover and thermal conditions to broader agroecological patterns. Together, these approaches form a tiered monitoring logic in which each method addresses the limitations of the others.

Seen in the wider East African context, this is especially important because smallholder agriculture remains central to food production and livelihoods, while still constrained by limited infrastructure, weak service systems, restricted access to technology, and the practical difficulty of observing highly variable farms in a timely way. The contribution of this thesis is therefore both methodological and applied: it shows how remote sensing can be organized into a monitoring framework that is scientifically credible, operationally realistic, and relevant to the conditions of smallholder cropping systems rather than designed only for large, uniform agricultural landscapes.

Overall, the thesis argues that the future of smallholder farm monitoring lies in integration, simplicity, and scalability. The most useful systems will not be those with the most advanced sensors alone, but those that can combine reliable field-level information with repeated wider-area observations in ways that institutions can actually use. In that sense, the broader conclusion is that remote sensing has

value not only as a technical tool for observation, but as a means of building timely, connected, and decision-relevant monitoring systems for smallholder agriculture.

6 References

Aalto, I. J., Maeda, E. E., Heiskanen, J., Aalto, E. K., & Pellikka, P. K. E. (2022). Strong influence of trees outside forest in regulating microclimate of intensively modified Afromontane landscapes. *Biogeosciences*, *19*(17), 4227–4247. https://doi.org/10.5194/bg-19-4227-2022

Aasen, H., Kirchgessner, N., Walter, A., & Liebisch, F. (2020). PhenoCams for Field Phenotyping: Using Very High Temporal Resolution Digital Repeated Photography to Investigate Interactions of Growth, Phenology, and Harvest Traits. *Frontiers in Plant Science*, *11*. https://doi.org/10.3389/fpls.2020.00593

Abdalla, M., Hastings, A., Cheng, K., Yue, Q., Chadwick, D., Espenberg, M., Truu, J., Rees, R. M., & Smith, P. (2019). A critical review of the impacts of cover crops on nitrogen leaching, net greenhouse gas balance and crop productivity. *Global Change Biology*, *25*(8), 2530–2543. https://doi.org/10.1111/gcb.14644

Abera, T., Heiskanen, J., Maeda, E., Odongo, V., & Pellikka, P. (2023). Impacts of land cover and management change on top-of-canopy and below-canopy temperatures in Southeastern Kenya. *Science of The Total Environment*, *874*, 162560. https://doi.org/10.1016/j.scitotenv.2023.162560

Al-Ali, Z. M., Abdullah, M. M., Asadalla, N. B., & Gholoum, M. (2020). A comparative study of remote sensing classification methods for monitoring and assessing desert vegetation using a UAV-based multispectral sensor. *Environmental Monitoring and Assessment*, *192*(6), 389. https://doi.org/10.1007/s10661-020-08330-1

Angelopoulou, T., Tziolas, N., Balafoutis, A., Zalidis, G., & Bochtis, D. (2019). Remote Sensing Techniques for Soil Organic Carbon Estimation: A Review. *Remote Sensing*, *11*(6), 676. https://doi.org/10.3390/rs11060676

Autio, A., Johansson, T., Motaroki, L., Minoia, P., & Pellikka, P. (2021). Constraints for adopting climate-smart agricultural practices among smallholder farmers in Southeast Kenya. *Agricultural Systems*, *194*, 103284. https://doi.org/10.1016/J.AGSY.2021.103284

Barnes, R. J., Dhanoa, M. S., & Lister, S. J. (1989). Standard Normal Variate Transformation and De-Trending of Near-Infrared Diffuse Reflectance Spectra. *Applied Spectroscopy*, *43*(5), 772–777. https://doi.org/10.1366/0003702894202201

Ben-Dor, E., & Banin, A. (1995). Quantitative analysis of convolved Thematic Mapper spectra of soils in the visible near-infrared and shortwave-infrared spectral regions (0·4–2·5 μm). *International Journal of Remote Sensing*, *16*(18), 3509–3528. https://doi.org/10.1080/01431169508954643

Breiman, L. (2001). Random Forests. *Machine Learning*, *45*(1), 5–32. https://doi.org/10.1023/A:1010933404324

Carlson, T. N., & Ripley, D. A. (1997). On the relation between NDVI, fractional vegetation cover, and leaf area index. *Remote Sensing of Environment*, *62*(3), 241–252. https://doi.org/10.1016/S0034-4257(97)00104-1

Chen, J., Liu, X., Du, S., Ma, Y., & Liu, L. (2020). Integrating SIF and Clearness Index to Improve Maize GPP Estimation Using Continuous Tower-Based Observations. *Sensors*, *20*(9). https://doi.org/10.3390/s20092493

Chen, X., Sun, Y., Qin, X., Cai, J., Cai, M., Hou, X., Yang, K., & Zhang, H. (2024). Assessing the Potential of UAV for Large-Scale Fractional Vegetation Cover Mapping with Satellite Data and Machine Learning. *Remote Sensing*, *16*(19), 3587. https://doi.org/10.3390/rs16193587

Chen, Y., Wang, J., Liu, G., Yang, Y., Liu, Z., & Deng, H. (2019). Hyperspectral Estimation Model of Forest Soil Organic Matter in Northwest Yunnan Province, China. *Forests*, *10*(3). https://doi.org/10.3390/f10030217

Conant, R. T., Ogle, S. M., Paul, E. A., & Paustian, K. (2011). Measuring and monitoring soil organic carbon stocks in agricultural lands for climate mitigation. *Frontiers in Ecology and the Environment*, *9*(3), 169–173. https://doi.org/10.1890/090153

Dare, P. M. (2005). Shadow Analysis in High-Resolution Satellite Imagery of Urban Areas. *Photogrammetric Engineering & Remote Sensing*, *71*(2), 169–177. https://doi.org/10.14358/PERS.71.2.169

DeFries, R. (2013). Remote Sensing and Image Processing. In *Encyclopedia of Biodiversity* (pp. 389–399). Elsevier. https://doi.org/10.1016/B978-0-12-384719-5.00383-X

Delavarpour, N., Koparan, C., Nowatzki, J., Bajwa, S., & Sun, X. (2021). A Technical Study on UAV Characteristics for Precision Agriculture Applications and Associated Practical Challenges. *Remote Sensing*, *13*(6). https://doi.org/10.3390/rs13061204

Diao, C., & Li, G. (2022). Near-Surface and High-Resolution Satellite Time Series for Detecting Crop Phenology. *Remote Sensing*, *14*(9), Article 9. https://doi.org/10.3390/rs14091957

Diao, C., Yang, Z., Gao, F., Zhang, X., & Yang, Z. (2021). Hybrid phenology matching model for robust crop phenological retrieval. *ISPRS Journal of Photogrammetry and Remote Sensing*, *181*, 308–326. https://doi.org/10.1016/j.isprsjprs.2021.09.011

Duan, T., Zheng, B., Guo, W., Ninomiya, S., Guo, Y., & Chapman, S. C. (2016). Comparison of ground cover estimates from experiment plots in cotton, sorghum and sugarcane based on images and ortho-mosaics captured by UAV. *Functional Plant Biology*, *44*(1), 169–183. https://doi.org/10.1071/FP16123

Erler, A., Riebe, D., Beitz, T., Löhmannsröben, H.-G., & Gebbers, R. (2020). Soil Nutrient Detection for Precision Agriculture Using Handheld Laser-Induced Breakdown Spectroscopy (LIBS) and Multivariate Regression Methods (PLSR, Lasso and GPR). *Sensors*, *20*(2). https://doi.org/10.3390/s20020418

Fawcett, D., Panigada, C., Tagliabue, G., Boschetti, M., Celesti, M., Evdokimov, A., Biriukova, K., Colombo, R., Miglietta, F., Rascher, U., & Anderson, K. (2020). Multi-Scale Evaluation of Drone-Based Multispectral Surface Reflectance and Vegetation Indices in Operational Conditions. *Remote Sensing*, *12*(3). https://doi.org/10.3390/rs12030514

Feng, Q., Liu, J., & Gong, J. (2015). UAV Remote Sensing for Urban Vegetation Mapping Using Random Forest and Texture Analysis. *Remote Sensing*, *7*(1), 1074–1094. https://doi.org/10.3390/rs70101074

Feng, Z., Cheng, Z., Ren, L., Liu, B., Zhang, C., Zhao, D., Sun, H., Feng, H., Long, H., Xu, B., Yang, H., Song, X., Ma, X., Yang, G., & Zhao, C. (2024). Real-time monitoring of maize phenology with the VI-RGS composite index using time-series UAV remote sensing images and meteorological data. *Computers and Electronics in Agriculture*, *224*, 109212. https://doi.org/10.1016/j.compag.2024.109212

Filippa, G., Cremonese, E., Migliavacca, M., Galvagno, M., Forkel, M., Wingate, L., Tomelleri, E., Morra di Cella, U., & Richardson, A. D. (2016). Phenopix: A R package for image-based vegetation phenology. *Agricultural and Forest Meteorology*, *220*, 141–150. https://doi.org/10.1016/j.agrformet.2016.01.006

Fischer, G. W., & Antoine, J. (with FAO & International Institute for Applied Systems Analysis). (1994). *Agro-ecological land resources assessment for agricultural development planning: A case study of Kenya: making land use choices for district planning*. Land and Water Development Division, Food and Agriculture Organization of the United Nations and International Institute for Applied Systems Analysis. https://digitallibrary.un.org/record/163012

Gao, F., Anderson, M. C., Zhang, X., Yang, Z., Alfieri, J. G., Kustas, W. P., Mueller, R., Johnson, D. M., & Prueger, J. H. (2017). Toward mapping crop progress at field scales through fusion of Landsat and MODIS imagery. *Remote Sensing of Environment*, *188*, 9–25. https://doi.org/10.1016/j.rse.2016.11.004

Gu, L., Post, W. M., Baldocchi, D. D., Black, T. A., Suyker, A. E., Verma, S. B., Vesala, T., & Wofsy, S. C. (2009). Characterizing the Seasonal Dynamics of Plant Community Photosynthesis Across a Range of Vegetation Types. In A. Noormets (Ed.), *Phenology of Ecosystem Processes: Applications in Global Change Research* (pp. 35–58). Springer. https://doi.org/10.1007/978-1-4419-0026-5_2

Guo, Y., Chen, S., Fu, Y. H., Xiao, Y., Wu, W., Wang, H., & Beurs, K. de. (2022). Comparison of Multi-Methods for Identifying Maize Phenology Using PhenoCams. *Remote Sensing*, *14*(2), Article 2. https://doi.org/10.3390/rs14020244

He, Y., Dosanjh, M., Shang, J., Liu, J., Drury, C. F., Yang, X., Yang, J., Dao, P. D., Axiotis, A., & Proctor, C. (2021). Mapping crop fractional green canopy cover using high spatial resolution thermal and optical remote sensing in southern Ontario, Canada1. *Geomatica*, *75*(3), 116–129. https://doi.org/10.1139/geomat-2021-0008

He, Y., Song, H., Pereira, A. G., & Gómez, A. H. (2005). Measurement and analysis of soil nitrogen and organic matter content using near-infrared spectroscopy techniques. *Journal of Zhejiang University-SCIENCE B*, *6*(11), 1081–1086. https://doi.org/10.1631/jzus.2005.B1081

Heinemann, S., Siegmann, B., Thonfeld, F., Muro, J., Jedmowski, C., Kemna, A., Kraska, T., Muller, O., Schultz, J., Udelhoven, T., Wilke, N., & Rascher, U. (2020). Land Surface Temperature Retrieval for Agricultural Areas Using a Novel UAV Platform Equipped with a Thermal Infrared and Multispectral Sensor. *Remote Sensing*, *12*(7). https://doi.org/10.3390/rs12071075

Hong, Y., Chen, S., Zhang, Y., Chen, Y., Yu, L., Liu, Y., Liu, Y., Cheng, H., & Liu, Y. (2018). Rapid identification of soil organic matter level via visible and near-infrared spectroscopy: Effects of two-dimensional correlation coefficient and extreme learning machine. *Science of The Total Environment*, *644*, 1232–1243. https://doi.org/10.1016/j.scitotenv.2018.06.319

Hufkens, K., Friedl, M., Sonnentag, O., Braswell, B. H., Milliman, T., & Richardson, A. D. (2012). Linking near-surface and satellite remote sensing measurements of deciduous broadleaf forest phenology. *Remote Sensing of Environment, Remote Sensing of Urban Environments*, *117*, 307–321. https://doi.org/10.1016/j.rse.2011.10.006

Jaetzold, R., Helmut, S., Berthold, H., & Chris, S. (2010). *Farm Management Handbook of Kenya VOL. II -Taita-Taveta County– Atlas of Agro-Ecological Zones, Soils and Fertilising (2nd ed.)*. Ministry of Agriculture, Kenya, in Cooperation with the German Agency for International Cooperation (GIZ).

Jaetzold, R., & Schmidt, H. (1983). *Farm Management Handbook of Kenya: Volume II: Natural Conditions and Farm Management Information; Part B Central Kenya (Rift Valley and Central Provinces)*. Verlag nicht ermittelbar.

Jandl, R., Rodeghiero, M., Martinez, C., Cotrufo, M. F., Bampa, F., van Wesemael, B., Harrison, R. B., Guerrini, I. A., Richter, D. deB, Rustad, L., Lorenz, K., Chabbi, A., & Miglietta, F. (2014). Current status, uncertainty and future needs in soil organic carbon monitoring. *Science of The Total Environment*, *468–469*, 376–383. https://doi.org/10.1016/j.scitotenv.2013.08.026

Jiang, J., Johansen, K., Tu, Y.-H., & McCabe, M. F. (2022). Multi-sensor and multi-platform consistency and interoperability between UAV, Planet CubeSat, Sentinel-2, and Landsat reflectance data. *GIScience & Remote Sensing*, *59*(1), 936–958. https://doi.org/10.1080/15481603.2022.2083791

Khangura, R., Ferris, D., Wagg, C., & Bowyer, J. (2023). Regenerative Agriculture—A Literature Review on the Practices and Mechanisms Used to Improve Soil Health. *Sustainability*, *15*(3), Article 3. https://doi.org/10.3390/su15032338

Klosterman, S. T., Hufkens, K., Gray, J. M., Melaas, E., Sonnentag, O., Lavine, I., Mitchell, L., Norman, R., Friedl, M. A., & Richardson, A. D. (2014). Evaluating remote sensing of deciduous forest phenology at multiple spatial scales using PhenoCam imagery. *Biogeosciences*, *11*(16), 4305–4320. https://doi.org/10.5194/bg-11-4305-2014

Kustas, W., & Anderson, M. (2009). Advances in thermal infrared remote sensing for land surface modeling. *Agricultural and Forest Meteorology, Environmental Biophysics - Tribute to John Norman*, *149*(12), 2071–2081. https://doi.org/10.1016/j.agrformet.2009.05.016

Lazaar, A., Mouazen, A. M., EL Hammouti, K., Fullen, M., Pradhan, B., Memon, M. S., Andich, K., & Monir, A. (2020). The application of proximal visible and near-infrared spectroscopy to estimate soil organic matter on the Triffa Plain of Morocco. *International Soil and Water Conservation Research*, *8*(2), 195–204. https://doi.org/10.1016/j.iswcr.2020.04.005

Li, L., Mu, X., Jiang, H., Chianucci, F., Hu, R., Song, W., Qi, J., Liu, S., Zhou, J., Chen, L., Huang, H., & Yan, G. (2023). Review of ground and aerial methods for vegetation cover fraction (fCover) and related quantities

estimation: Definitions, advances, challenges, and future perspectives. *ISPRS Journal of Photogrammetry and Remote Sensing*, *199*, 133–156. https://doi.org/10.1016/j.isprsjprs.2023.03.020

Li, Z.-L., Tang, B.-H., Wu, H., Ren, H., Yan, G., Wan, Z., Trigo, I. F., & Sobrino, J. A. (2013). Satellite-derived land surface temperature: Current status and perspectives. *Remote Sensing of Environment*, *131*, 14–37. https://doi.org/10.1016/j.rse.2012.12.008

Liu, Y., Bachofen, C., Wittwer, R., Silva Duarte, G., Sun, Q., Klaus, V. H., & Buchmann, N. (2022). Using PhenoCams to track crop phenology and explain the effects of different cropping systems on yield. *Agricultural Systems*, *195*, 103306. https://doi.org/10.1016/j.agsy.2021.103306

Liu, Z., Hu, H., Yu, H., Yang, X., Yang, H., Ruan, C., Wang, Y., & Tang, J. (2015). Relationship between leaf physiologic traits and canopy color indices during the leaf expansion period in an oak forest. *Ecosphere*, *6*(12), 1–9. https://doi.org/10.1890/ES14-00452.1

Lobell, D. B., Asner, G. P., Ortiz-Monasterio, J. I., & Benning, T. L. (2003). Remote sensing of regional crop production in the Yaqui Valley, Mexico: Estimates and uncertainties. *Agriculture, Ecosystems & Environment*, *94*(2), 205–220. https://doi.org/10.1016/S0167-8809(02)00021-X

Lobell, D. B., Hammer, G. L., McLean, G., Messina, C., Roberts, M. J., & Schlenker, W. (2013). The critical role of extreme heat for maize production in the United States. *Nature Climate Change*, *3*(5), 497–501. https://doi.org/10.1038/nclimate1832

Lopatin, J., Dolos, K., Kattenborn, T., & Fassnacht, F. E. (2019). How canopy shadow affects invasive plant species classification in high spatial resolution remote sensing. *Remote Sensing in Ecology and Conservation*, *5*(4), 302–317. https://doi.org/10.1002/rse2.109

Madari, B. E., Reeves, J. B., Machado, P. L. O. A., Guimarães, C. M., Torres, E., & McCarty, G. W. (2006). Mid- and near-infrared spectroscopic assessment of soil compositional parameters and structural indices in two Ferralsols. *Geoderma*, *136*(1), 245–259. https://doi.org/10.1016/j.geoderma.2006.03.026

Mahmud, A., Hoque, A., Tuure, J., Alakukku, L., Mäkelä, P., Wachiye, S., Mjomba, M., Pellikka, P., & Heiskanen, J. (2026b). Dataset from "Integrating field camera imagery for monitoring maize phenology, biophysical traits, and agroclimatic factors in smallholder farms" [Dataset]. In Computers and Electronics in Agriculture: Volume 240 (p. 111161). Zenodo. https://doi.org/10.5281/zenodo.21114860

Mahmud, A., Luotamo, M., Karhu, K., Pellikka, P., Tuure, J., & Heiskanen, J. (2026a). Dataset from "Comparison of field and imaging spectroscopy to optimize soil organic carbon and nitrogen estimation in field laboratory conditions" [Dataset]. In CATENA: Volume 243 (p. 108180). Zenodo. https://doi.org/10.5281/zenodo.20702109Martens, H., & Naes, T. (1992). *Multivariate calibration*. John Wiley & Sons.

Martin, P. D., Malley, D. F., Manning, G., & Fuller, L. (2002). Determination of soil organic carbon and nitrogen at the field level using near-infrared spectroscopy. *Canadian Journal of Soil Science*, *82*(4), 413–422. https://doi.org/10.4141/S01-054

Martínez Prentice, R., Villoslada, M., Ward, R. D., Bergamo, T. F., Joyce, C. B., & Sepp, K. (2024). Synergistic use of Sentinel-2 and UAV-derived data for plant fractional cover distribution mapping of coastal meadows with digital

elevation models. *Biogeosciences*, *21*(6), 1411–1431. https://doi.org/10.5194/bg-21-1411-2024

Meireles, J. E., Schweiger, A. K., & Cavender-Bares, J. (2023). Spectrolab: Class and Method s for Spectral Data(0.0. 18). *Computer Software*.

Miloš, B., & Bensa, A. (2017). Prediction of soil organic carbon using VIS-NIR spectroscopy: Application to Red Mediterranean soils from Croatia. *Eurasian Journal of Soil Science*, *6*(4), 365–373. https://doi.org/10.18393/ejss.319208

Morellos, A., Pantazi, X.-E., Moshou, D., Alexandridis, T., Whetton, R., Tziotzios, G., Wiebensohn, J., Bill, R., & Mouazen, A. M. (2016). Machine learning based prediction of soil total nitrogen, organic carbon and moisture content by using VIS-NIR spectroscopy. *Biosystems Engineering, Proximal Soil Sensing – Sensing Soil Condition and Functions*, *152*, 104–116. https://doi.org/10.1016/j.biosystemseng.2016.04.018

Mulla, D. J. (2013). Twenty five years of remote sensing in precision agriculture: Key advances and remaining knowledge gaps. *Biosystems Engineering, Special Issue: Sensing Technologies for Sustainable Agriculture*, *114*(4), 358–371. https://doi.org/10.1016/j.biosystemseng.2012.08.009

Nakalembe, C., Becker-Reshef, I., Bonifacio, R., Hu, G., Humber, M. L., Justice, C. J., Keniston, J., Mwangi, K., Rembold, F., Shukla, S., Urbano, F., Whitcraft, A. K., Li, Y., Zappacosta, M., Jarvis, I., & Sanchez, A. (2021). A review of satellite-based global agricultural monitoring systems available for Africa. *Global Food Security*, *29*, 100543. https://doi.org/10.1016/j.gfs.2021.100543

Nocita, M., Stevens, A., Van Wesemael, B., Aitkenhead, M., Bachmann, M., Barthès, B., Ben Dor, E., Brown, D. J., Clairotte, M., Csorba, A., Dardenne, P., Demattê, J. A. M., Genot, V., Guerrero, C., Knadel, M., Montanarella, L., Noon, C., Ramirez-Lopez, L., Robertson, J., … Wetterlind, J. (2015). Soil Spectroscopy: An Alternative to Wet Chemistry for Soil Monitoring. In *Advances in Agronomy* (Vol. 132, pp. 139–159). Elsevier. https://doi.org/10.1016/bs.agron.2015.02.002

Otsu, N. (1979). A Threshold Selection Method from Gray-Level Histograms. *IEEE Transactions on Systems, Man, and Cybernetics*, *9*(1), 62–66. https://doi.org/10.1109/TSMC.1979.4310076

Pellikka, P. K. E., Clark, B. J. F., Gosa, A. G., Himberg, N., Hurskainen, P., Maeda, E., Mwang'ombe, J., Omoro, L. M. A., & Siljander, M. (2013). Agricultural Expansion and Its Consequences in the Taita Hills, Kenya. In *Developments in Earth Surface Processes* (Vol. 16, pp. 165–179). Elsevier. https://doi.org/10.1016/B978-0-444-59559-1.00013-X

Pellikka, P., Luotamo, M., Sädekoski, N., Hietanen, J., Vuorinne, I., Räsänen, M., Heiskanen, J., Siljander, M., Karhu, K., & Klami, A. (2023). Tropical altitudinal gradient soil organic carbon and nitrogen estimation using Specim IQ portable imaging spectrometer. *Science of The Total Environment*, *883*, 163677. https://doi.org/10.1016/j.scitotenv.2023.163677

Poeplau, C., & Don, A. (2015). Carbon sequestration in agricultural soils via cultivation of cover crops – A meta-analysis. *Agriculture, Ecosystems & Environment*, *200*, 33–41. https://doi.org/10.1016/j.agee.2014.10.024

Prescott, C. E., Rui, Y., Cotrufo, M. F., & Grayston, S. J. (2021). Managing plant surplus carbon to generate soil organic matter in regenerative agriculture.

Journal of Soil and Water Conservation, *76*(6), 99A-104A. https://doi.org/10.2489/jswc.2021.0920A

Rasmussen, C. E. (2004). Gaussian Processes in Machine Learning. In O. Bousquet, U. von Luxburg, & G. Rätsch (Eds.), *Advanced Lectures on Machine Learning: ML Summer Schools 2003, Canberra, Australia, February 2—14, 2003, Tübingen, Germany, August 4—16, 2003, Revised Lectures* (pp. 63–71). Springer. https://doi.org/10.1007/978-3-540-28650-9_4

Rhodes, C. J. (2017). The Imperative for Regenerative Agriculture. *Science Progress*, *100*(1), 80–129. https://doi.org/10.3184/003685017X14876775256165

Ricciardi, V., Ramankutty, N., Mehrabi, Z., Jarvis, L., & Chookolingo, B. (2018). How much of the world's food do smallholders produce? *Global Food Security*, *17*, 64–72. https://doi.org/10.1016/j.gfs.2018.05.002

Richardson, A. D., Braswell, B. H., Hollinger, D. Y., Jenkins, J. P., & Ollinger, S. V. (2009). Near-surface remote sensing of spatial and temporal variation in canopy phenology. *Ecological Applications*, *19*(6), 1417–1428. https://doi.org/10.1890/08-2022.1

Richardson, A. D., Jenkins, J. P., Braswell, B. H., Hollinger, D. Y., Ollinger, S. V., & Smith, M.-L. (2007). Use of digital webcam images to track spring green-up in a deciduous broadleaf forest. *Oecologia*, *152*(2), 323–334. https://doi.org/10.1007/s00442-006-0657-z

Riihimäki, H., Luoto, M., & Heiskanen, J. (2019). Estimating fractional cover of tundra vegetation at multiple scales using unmanned aerial systems and optical satellite data. *Remote Sensing of Environment*, *224*, 119–132. https://doi.org/10.1016/j.rse.2019.01.030

Rose, M. B., Mills, M., Franklin, J., & Larios, L. (2023). Mapping Fractional Vegetation Cover Using Unoccupied Aerial Vehicle Imagery to Guide Conservation of a Rare Riparian Shrub Ecosystem in Southern California. *Remote Sensing*, *15*(21), 5113. https://doi.org/10.3390/rs15215113

Salami, A., Kamara, A. B., & Brixiova, Z. (2010). Smallholder Agriculture in East Africa: Trends, Constraints and Opportunities. *African Development Bank Group, Working Paper No. 105*. https://www.afdb.org/en/documents/document/working-paper-105-smallholder-agriculture-in-east-africa-trends-constraints-and-opportunities-20266

Sandholt, I., Rasmussen, K., & Andersen, J. (2002). A simple interpretation of the surface temperature/vegetation index space for assessment of surface moisture status. *Remote Sensing of Environment, Recent Advances in Remote Sensing of Biophysical Variables*, *79*(2), 213–224. https://doi.org/10.1016/S0034-4257(01)00274-7

Savitzky, Abraham., & Golay, M. J. E. (1964). Smoothing and Differentiation of Data by Simplified Least Squares Procedures. *Analytical Chemistry*, *36*(8), 1627–1639. https://doi.org/10.1021/ac60214a047

Sinfield, J. V., Fagerman, D., & Colic, O. (2010). Evaluation of sensing technologies for on-the-go detection of macro-nutrients in cultivated soils. *Computers and Electronics in Agriculture*, *70*(1), 1–18. https://doi.org/10.1016/j.compag.2009.09.017

Sonnentag, O., Hufkens, K., Teshera-Sterne, C., Young, A. M., Friedl, M., Braswell, B. H., Milliman, T., O'Keefe, J., & Richardson, A. D. (2012). Digital repeat

photography for phenological research in forest ecosystems. *Agricultural and Forest Meteorology*, *152*, 159–177. https://doi.org/10.1016/j.agrformet.2011.09.009

Stenberg, B., Viscarra Rossel, R. A., Mouazen, A. M., & Wetterlind, J. (2010). Visible and Near Infrared Spectroscopy in Soil Science. In *Advances in Agronomy* (Vol. 107, pp. 163–215). Elsevier. https://doi.org/10.1016/S0065-2113(10)07005-7

Sun, D., & Kafatos, M. (2007). Note on the NDVI-LST relationship and the use of temperature-related drought indices over North America. *Geophysical Research Letters*, *34*(24). https://doi.org/10.1029/2007GL031485

SVC. (2020). *SVC HR i Series User Manual Revision 1.17*. Spectra Vista Corporation.

Tan, B., You, W., Tian, S., Xiao, T., Wang, M., Zheng, B., & Luo, L. (2022). Soil Nitrogen Content Detection Based on Near-Infrared Spectroscopy. *Sensors*, *22*(20). https://doi.org/10.3390/s22208013

Tan, S. S. X., & Kuebbing, S. E. (2023). A synthesis of the effect of regenerative agriculture on soil carbon sequestration in Southeast Asian croplands. *Agriculture, Ecosystems & Environment*, *349*, 108450. https://doi.org/10.1016/j.agee.2023.108450

Tibshirani, R. (1996). Regression Shrinkage and Selection Via the Lasso. *Journal of the Royal Statistical Society: Series B (Methodological)*, *58*(1), 267–288. https://doi.org/10.1111/j.2517-6161.1996.tb02080.x

U.S. Geological Survey. (2024). *Landsat 8-9 Collection 2 Level 2 Science Product Guide*.

USGS. (2019). *Landsat 8 (L8) Data Users Handbook*. U.S. Geological Survey (USGS). https://d9-wret.s3.us-west-2.amazonaws.com/assets/palladium/production/s3fs-public/atoms/files/LSDS-1574_L8_Data_Users_Handbook-v5.0.pdf

USGS. (2022). *Landsat 9 Data Users Handbook*. U.S. Geological Survey (USGS). https://d9-wret.s3.us-west-2.amazonaws.com/assets/palladium/production/s3fs-public/media/files/LSDS-2082_L9-Data-Users-Handbook_v1.pdf

Vibhute, A. D., Kale, K. V., Gaikwad, S. V., & Dhumal, R. K. (2020). Estimation of soil nitrogen in agricultural regions by VNIR reflectance spectroscopy. *SN Applied Sciences*, *2*(9), 1523. https://doi.org/10.1007/s42452-020-03322-9

Viscarra Rossel, R. A., Walvoort, D. J. J., McBratney, A. B., Janik, L. J., & Skjemstad, J. O. (2006). Visible, near infrared, mid infrared or combined diffuse reflectance spectroscopy for simultaneous assessment of various soil properties. *Geoderma*, *131*(1), 59–75. https://doi.org/10.1016/j.geoderma.2005.03.007

Vrieling, A., Meroni, M., Darvishzadeh, R., Skidmore, A. K., Wang, T., Zurita-Milla, R., Oosterbeek, K., O'Connor, B., & Paganini, M. (2018). Vegetation phenology from Sentinel-2 and field cameras for a Dutch barrier island. *Remote Sensing of Environment*, *215*, 517–529. https://doi.org/10.1016/j.rse.2018.03.014

Wei, F., Wang, S., Fu, B., Wang, L., Liu, Y. Y., & Li, Y. (2019). African dryland ecosystem changes controlled by soil water. *Land Degradation & Development*, *30*(13), 1564–1573. https://doi.org/10.1002/ldr.3342

Weiss, M., Jacob, F., & Duveiller, G. (2020). Remote sensing for agricultural applications: A meta-review. *Remote Sensing of Environment*, *236*, 111402. https://doi.org/10.1016/J.RSE.2019.111402

Weng, Q., Lu, D., & Schubring, J. (2004). Estimation of land surface temperature–vegetation abundance relationship for urban heat island studies. *Remote Sensing of Environment*, *89*(4), 467–483. https://doi.org/10.1016/j.rse.2003.11.005

Wijewardane, N. K., Ge, Y., Wills, S., & Loecke, T. (2016). Prediction of Soil Carbon in the Conterminous United States: Visible and Near Infrared Reflectance Spectroscopy Analysis of the Rapid Carbon Assessment Project. *Soil Science Society of America Journal*, *80*(4), 973–982. https://doi.org/10.2136/sssaj2016.02.0052

Woodcock, C. E., & Strahler, A. H. (1987). The factor of scale in remote sensing. *Remote Sensing of Environment*, *21*(3), 311–332. https://doi.org/10.1016/0034-4257(87)90015-0

Xiao, S., & He, Y. (2019). Application of Near-infrared Spectroscopy and Multiple Spectral Algorithms to Explore the Effect of Soil Particle Sizes on Soil Nitrogen Detection. *Molecules*, *24*(13). https://doi.org/10.3390/molecules24132486

Yang, S., Li, S., Zhang, B., Yu, R., Li, C., Hu, J., Liu, S., Cheng, E., Lou, Z., & Peng, D. (2023). Accurate estimation of fractional vegetation cover for winter wheat by integrated unmanned aerial systems and satellite images. *Frontiers in Plant Science*, *14*. https://doi.org/10.3389/fpls.2023.1220137

Zhang, H., Cai, J., Cai, M., Chen, X., Sun, Y., Chen, K., Cao, S., & Ren, J. (2025). An upscaling framework for estimating regional-scale fractional cover of Chinese fir (FCCF) by integrating UAV and satellite images. *International Journal of Digital Earth*, *18*(1), 2510570. https://doi.org/10.1080/17538947.2025.2510570

Zhao, Q., & Qu, Y. (2024). The Retrieval of Ground NDVI (Normalized Difference Vegetation Index) Data Consistent with Remote-Sensing Observations. *Remote Sensing*, *16*(7), Article 7. https://doi.org/10.3390/rs16071212